ORIGINAL ARTICLE

Radio-anatomical Study of the Greater Palatine Canal and the Pterygopalatine Fossa in a Lebanese Population: A Consideration for Maxillary Nerve Block

Georges Aoun, Ibrahim Nasseh[1], Sayde Sokhn[1]

Departments of Oral Pathology and Diagnosis and [1]Dentomaxillofacial Radiology and Imaging, School of Dentistry, Lebanese University, Beirut, Lebanon

Address for correspondence:
Dr. Georges Aoun,
Department of Oral Pathology and Diagnosis, School of Dentistry, Lebanese University, Beirut, Lebanon.
E-mail: aoungeorges@yahoo.com

ABSTRACT

Aim: The aim of this study was to describe the morphology of the component, greater palatine canal-pterygopalatine fossa (GPC-PPF), in a Lebanese population using cone-beam computed tomography (CBCT) technology. **Materials and Methods:** CBCT images of 79 Lebanese adult patients (38 females and 41 males) were included in this study, and a total of 158 cases were evaluated bilaterally. The length and path of the GPCs-PPFs were determined, and the data obtained analyzed statistically. **Results:** In the sagittal plane, of all the GPCs-PPFs assessed, the average length was 35.02 mm on the right and 35.01 mm on the left. The most common anatomic path consisted in the presence of a curvature resulting in an internal narrowing whose average diameter was 2.4 mm on the right and 2.45 mm on the left. The mean diameter of the upper opening was 5.85 mm on the right and 5.82 mm on the left. As for the lower opening corresponding to the greater palatine foramen, the right and left average diameters were 6.39 mm and 6.42 mm, respectively. **Conclusion:** Within the limits of this study, we concluded that throughout the Lebanese population, the GPC-PPF path is variable with a predominance of curved one (77.21% [122/158] in both the right and left sides); however, the GPC-PPF length does not significantly vary according to gender and side.

Key words: Cone-beam computed tomography, greater palatine canal, greater palatine foramen, Lebanese population, pterygopalatine fossa

Access this article online

Quick Response Code:

Website:
www.clinicalimagingscience.org

DOI:
10.4103/2156-7514.190862

INTRODUCTION

The pterygopalatine fossa (PPF) is a paired, inversed cone-shaped depression, located deep in the infratemporal fossa and posterior to the maxilla.[1] It communicates with several other regions via different passageways (fissures, foramina, and canals). Its rather small dimension, combined with the numerous components within it, clearly marks the PPF as a complex region.[2]

The PPF contains the parasympathetic pterygopalatine ganglion, the maxillary nerve (CN V2) and artery, their branches, and the maxillary vein.[3] The greater palatine canal (GPC) extends from the inferior aspect of the PPF to the greater palatine foramen (GPF) at the hard palate.

The GPC approach to block of the CN V2 by injecting local anesthesia in the PPF achieves profound anesthesia of the hemimaxilla including bone, soft tissue, and teeth,[4,5] the midface skin,[6] the nasal cavity, and sinus (during septorhinoplasty and endoscopic sinus surgery).[7-9]

As described by Malamed and Trieger,[10] this technique consists of the insertion of a 25-gauge anesthesia needle, 32 mm in length, through the GPF. The needle is introduced slowly at an angle of 45° to the big axis of the hard palate in the GPC to almost a depth of 32 mm in adults.

One point eight milliliters (1.8 ml) of local anesthetic is injected without compression to avoid the possibility of tissue necrosis. Aspiration is indispensable before injection; if blood or air bubbles are aspirated, the needle is removed, redirected, and reinserted at a different angle.

However, with time, this technique became less popular after the numerous complications subsequent to technical difficulties, mainly due to the poor acquaintance of practitioners with the region anatomy.[11,12]

Among these complications, the persistent paresthesia resulting from CN V2 trauma or local hematoma formation,[13] the diplopia due to the anesthetic diffusion into the orbit through the inferior orbital fissure, reaching and blocking of the abducens nerve (responsible of the innervations of one of the eye muscles, the lateral rectus),[13] and the ptosis from anesthetizing the superior branch of the oculomotor nerve innervating the levator muscle of the upper eyelid.[5]

More severe complications can occur such as the injury and/or injection of the infraorbital nerve by accidental penetration of the orbit, a temporary blindness associated with the vasoconstriction of the ophthalmic artery and unconsciousness due to the dissemination of the anesthetic into the middle cranial fossa via the foramen rotundum.[14]

In this respect, knowledge of the anatomy and length of the GPC-PPF is imperative to avoid the said problems. Indeed, nowadays, the benefit resulting from the technological advancement of the imaging techniques such as cone-beam computed tomography (CBCT) provides alternatives for detailed and accurate assessments.[4,15]

The purpose of this investigation was to analyze the morphology of the GPC-PPF using CBCT data obtained from Lebanese adult population.

MATERIALS AND METHODS

The study was conducted on CBCT scans of Lebanese adult patients who were referred to a specialized maxillofacial imaging center for multiple indications (e.g., impacted teeth, sinus diagnosis, implant planning). The scans were acquired using the PaX-Zenith3D© machine (Vatech Co. Ltd., Yongin-Si, Republic of Korea) with technical parameters ranged between 70 and 100 kVp and 7–15 mA, with an exposure time of 20–35 s and medium to large field of view according to the clinical case, in respect to the "As Low As Reasonably Achievable" principle.

All patients were informed in advance that the scans might be anonymously used for research reasons later and their consent was obtained. The study got the approval of the Center Institutional Board.

The inclusion criteria included the age of 18 years or older and the absence of any pathological changes or deformities in the region of the maxilla.

Seventy-nine CBCT images of 41 males and 38 females (a total of 158 cases bilaterally) with an age ranging from 18 to 67 years met the inclusion criteria and were included in this study.

The images were assessed by one oral and maxillofacial radiologist having more than 10 years of experience, who analyzed the lengths and anatomic paths of the right and left GPCs-PPFs in both coronal and sagittal planes.

Evaluating the images extended over three sessions of an average of twenty cases each. A 5-day period existed between the sessions.

To assess measurement error, all measurements were repeated by the examiner 2 weeks after the first readings without having in hands the initial results. In the case of any discrepancies, the mean of the two values was recorded.

To evaluate the length, we considered the higher bony aspect of the PPF as the upper limit, and the GPF on the inferior surface of the hard palate as the lower one.

The palatal soft tissue thickness was not included in the study.

The observations were made as follows:
1. Mean length of the GPC-PPF and the upper and lower openings diameter: The axial cut was tilted to see the path of GPC-PPF in the sagittal cut where we traced two lines: One at the upper bony border and the second at the lower part to measure the diameter of both openings; the length was then measured in millimeters from these marks [Figure 1]
2. Path of the GPC-PPF: The pathway of the GPC-PPF was recorded as the description of the descending length tracing lines. It was classified into two categories: straight or curved. In the later case, the precise location of the curvature was noted: upper, middle, or lower [Figures 1-4].

Descriptive statistics of age, gender, openings diameter (upper and lower), and lengths of the GPCs-PPFs were calculated and compared between the left and right sides using the paired *t*-test and between males and females using the independent *t*-test. The Chi-square test of association was used to test the difference in percent distribution of the internal curvatures between the right and left sides and between genders. Fisher's exact test was applied whenever the expected cell count requirement of 5 was violated. The SPSS® statistics 20.0 statistical package (IBM®, USA) was used to carry out all statistical analyses. Statistical significance was set at 0.05.

RESULTS

Descriptive statistics

The anatomic characteristics of the GPC-PPF varied significantly among the assessed adult population (mean age 33.59 ± 15.42 years). The length ranged from a minimum of 24.22 to a maximum of 45.30 mm [Table 1]. The mean diameter of the upper opening was 5.83 mm whereas the average value for the diameter of the lower opening was 6.40 mm. Values for the diameter of the curvature lied in a more narrow range; between 1.1 and 3.40 mm (average 2.42 mm) and the majority of curvatures were located in the middle (60.76% [48/79] on the right,

Table 1: Descriptive statistics of subjects age, greater palatine canal upper and lower openings, and intra-canal curvature diameters and length

|	*n*	Minimum	Maximum	Mean ± SD
Age (years)	79	18	67	33.59 ± 15.42
Diameter upper opening (mm)				
Right	79	3.6	9.7	5.85 ± 1.24
Left	79	3.22	9.8	5.82 ± 1.27
Diameter lower opening (mm)				
Right	79	4	9.7	6.39 ± 1.28
Left	79	4.4	9.2	6.42 ± 1.09
Diameter of curvature (mm)				
Right	64	1.1	4	2.4 ± 0.71
Left	59	1.2	3.4	2.45 ± 0.55
GPC length (mm)				
Right	79	24.22	45.3	35.02 ± 3.89
Left	79	24.52	44.3	35.01 ± 3.82

SD: Standard deviation, GPC: Greater palatine canal
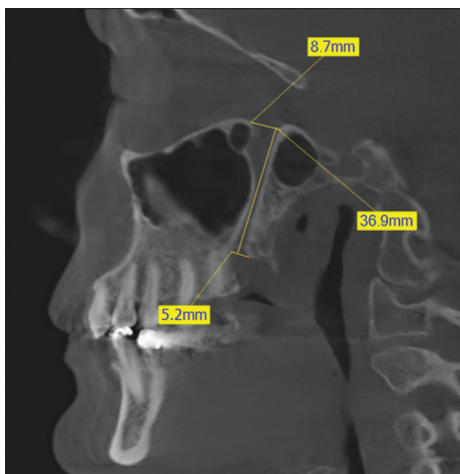
Figure 1: A cone-beam computed tomography, sagittal cut at the level of the pterygopalatine fossa illustrating the method of measuring for the greater palatine canal-pterygopalatine fossa component: (1) the length (36.9 mm) and path which is in this case straight (descending yellow line), (2) the lower limit and opening corresponding to the greater palatine foramen (5.2 mm in anteroposterior direction), and (3) the upper limit and opening (8.7 mm) as considered by our study (the higher radiologic bony aspect of the pterygopalatine fossa).
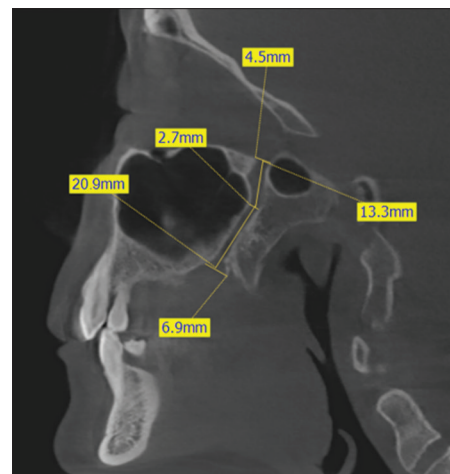
Figure 2: A cone-beam computed tomography, sagittal cut at the level of the pterygopalatine fossa illustrating the method of measuring for the greater palatine canal-pterygopalatine fossa component: (1) the length (34.2 mm) and the path which are in this case curved with an upper-located internal curvature of 2.7 mm diameter, (2) the lower limit and opening corresponding to the greater palatine foramen (6.9 mm in anteroposterior direction), and (3) the upper limit and opening (4.5 mm) as considered by our study (the higher radiologic bony aspect of the pterygopalatine fossa).
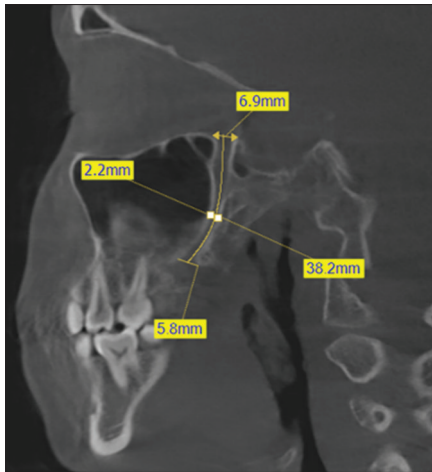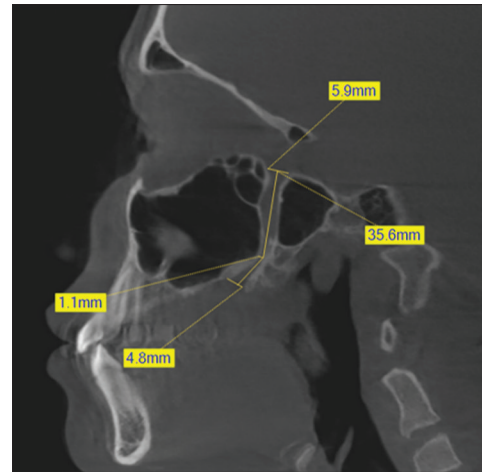
Figure 3: A cone-beam computed tomography, sagittal cut at the level of the pterygopalatine fossa illustrating the method of measuring for the greater palatine canal-pterygopalatine fossa component: (1) the length (38.2 mm) and the path which is in this case curved with a middle-located internal curvature of 2.2 mm diameter, (2) the lower limit and opening corresponding to the greater palatine foramen (5.8 mm in anteroposterior direction), and (3) the upper limit and opening (6.9 mm) as considered by our study (the higher radiologic bony aspect of the pterygopalatine fossa).

Figure 4: A cone-beam computed tomography, sagittal cut at the level of the pterygopalatine fossa illustrating the method of measuring for the pterygopalatine fossa component: (1) the length (35.6 mm) and the path which are in this case curved with a lower-located internal curvature of 1.1 mm diameter, (2) the lower limit and opening corresponding to the greater palatine foramen (4.8 mm in anteroposterior direction), and (3) the upper limit and opening (5.9 mm) as considered by our study (the higher radiologic bony aspect of the pterygopalatine fossa).

49.37% [39/79] on the left; Table 2). Curvatures positioned in the lower third were a rare occurrence (3.16% [5/158] of the total sample) and in slightly less than a quarter, the curvature was absent (22.79% [36/158] of combined sample; Table 2).

Side-related differences

There were no side-related differences in GPC-PPF dimensions [Table 3]. The average diameters of the upper and lower openings differed nonsignificant amounts of 0.03 and 0.04 mm between the right and left sides ($P = 0.84$ and 0.76, respectively). Differences in mean curvature diameter and length were an even smaller 0.02 and 0.01 mm, respectively ($P = 0.82$ and 0.97).

The location of the internal curvature, on the other hand, did display statistically significant side-related differences ($\chi^2 = 27.467$, $P < 0.001$; Table 4). While the proportion of middle-located curvatures approached two-thirds on the right side (60.76% [48/79]), this occurred in only around half the canals on the left side (49.37% [39/79]). This difference translated into a higher proportion of GPCs-PPFs lacking a curvature on the left than on the right side (26.58% [21/79] compared to only 18.99% [15/79]) and a slightly higher percentage with GPCs-PPFs in the upper third (20.25% [16/79] on the left compared to 17.72% [14/79] on the right). The same trend was also noted with respect to curvatures located in the lower third, but the proportion of these was low on both sides (3.8% [3/79] on the left compared to 2.5% [2/79] on the right).

Table 2: Distribution of the location of the curvature inside the greater palatine canal (n=79)

Position of the curvature	Right, n (%)	Left, n (%)	Combined, n (%)
Lower	2 (2.53)	3 (3.8)	5 (3.16)
Middle	48 (60.76)	39 (49.37)	87 (55.06)
Upper	14 (17.72)	16 (20.25)	30 (18.99)
Absence	15 (18.99)	21 (26.58)	36 (22.79)

Gender differences

The assessed sample was almost equally distributed by gender (51.89% males, $n = 41$ out of 79). Only the diameters of the upper and lower openings displayed statistically significant differences in the comparison between males and females [Table 5]. The difference was more pronounced on the right, the diameter of the upper opening being on the average 1.05 mm larger in males ($P < 0.001$) and the lower larger by 0.8 mm ($P = 0.005$). Left-side openings were also larger in males, but to a smaller extent (upper: 0.57 mm mean difference, $P = 0.048$; lower: 0.48 mm mean difference, $P = 0.049$). Curvature diameter and GPCs-PPFs length on both sides were comparable in males and females ($P \geq 0.160$). Similarly, the internal curvature location displayed no gender-related differences on either side (right: $P = 0.859$; left: $P = 0.108$; Table 6).

DISCUSSION

The maxillary nerve block through the GPC-PPF is a very advantageous technique. However, due to many difficulties causing potential complications resulting from poor knowledge of the anatomy of the region, a good

Table 3: Distribution of the diameter openings upper and lower, the curvature diameter and the canal length, by anatomical right or left side

| | Mean ± SD | | Difference (right-left) | | |
	Right	Left	Mean	t	P
Diameter opening upper (mm)	5.85 ± 1.24	5.82 ± 1.27	0.03	0.20	0.84
Diameter opening lower (mm)	6.38 ± 1.28	6.42 ± 1.09	−0.04	−0.31	0.76
Diameter curvature (mm)	2.43 ± 0.71	2.41 ± 0.53	0.02	0.23	0.82
Canal length (mm)	35.02 ± 3.89	35.01 ± 3.82	0.01	0.04	0.97

SD: Standard deviation

Table 4: Percent distribution of the intracanal curvature by anatomical right or left side (n=79)

| Right | Left, n (%) | | | | Total |
	Lower	Middle	Absent	Upper	
Lower	0	2 (2.5)	0	0	2 (2.5)
Middle	2 (2.5)	30 (38)	10 (12.7)	6 (7.6)	48 (60.8)
Absence	1 (1.3)	2 (2.5)	10 (12.7)	2 (2.5)	15 (19)
Upper	0	5 (6.3)	1 (1.3)	8 (10.1)	14 (17.7)
Total	3 (3.8)	39 (49.4)	21 (26.6)	16 (20.3)	79 (100)

χ^2 (Fisher's exact)=27.467, P<0.001

investigation before the maneuver is essential. In this context, a CBCT is indicated.

Many researchers studied the GPC-PPF in different ways and populations. Some of them on dry skulls,[6,16] the others using the imaging technology (CT, CBCT…).[3,4,7,17-19]

Concerning the GPC length, it was either evaluated as an independent entity from the PPF, [3,13,19,20] or considered as a GPC-PPF extending superiorly from different landmarks in the PPF, such as the foramen rotundum[6] or the vidian canal,[4,7,17,21] to the GPF inferiorly.

In our study conducted on Lebanese adults using CBCT, we opted for the upper radiologic bony aspect of the PPF as the upper limit of the GPC-PPF component. The average length was 35.015 ± 3.85 mm ranging from 24.22 to 45.30 mm.

Douglas and Wormald[13] concluded after CT scan evaluation of 22 cadaver heads that the average length of the GPC is 18.5 mm ranging from 17.9 to 19.1 mm, and the average height of the PPF is 21.6 mm (20.7–22.5 mm) making GPC-PPF mean 40.1 mm.

For Hwang et al.,[3] who investigated the morphology of the GPF, GPC, and PPF using CT scan measurements of fifty patients, the mean GPC length was found to be 13.8 ± 2.0 mm, and the mean PPF height 21.0 ± 3.4 mm making GPC-PPF average as 34.8 mm.

Our results that are consistent with the ones of Hwang et al., show a small difference with the findings of Douglas and Wormald maybe due to ethnicity reason or the limited size of their sample compared to ours.

As for the studies conducted by Howard-Swirzinski et al.,[4] Tomaszewska et al.,[7] and Sheikhi et al.,[17] their results

cannot be compared with ours since they adopted a different technique to measure the GPC-PPF (the opening of the vidian canal situated in the center of the PPF was taken as the upper limit for measurement).

In the literature, the suggested length of insertion of the anesthetic needle into the GPC is situated between 32 and 39 mm for CN V2 block.[11-13,18] The results of our study fell within previously recognized standards and ranges.

Concerning the GPC-PPF shape, two different path types were described, straight, or curved with one or two internal curvatures situated at different levels.[4,7,17,21] Those path types were evaluated in both sagittal and coronal planes.[4,7,17]

In our sample assessed in sagittal plane [Table 2], we found 77.2% (122/158) of curved GPCs-PPFs (presenting one curvature) with 3.16% (5/158) of the curvatures located in the lower part [Figure 4], 18.99% (30/158) in the upper part [Figure 2], and 55.06% (87/158) in the middle [Figure 3]. Thus, in our study, the majority of the GPCs-PPFs were curved, and only 22.79% (36/158) were straight [Figure 1].

These results cannot be compared with others due to the difference in the landmarks taken in the PPF as the upper limit of the component.

For the lower GPC opening (GPF) diameter measured anteroposteriorly, the results of this study (average 6.40 mm) like our previous one (average 5.67 mm),[22] confirm that the mean diameter of GPF in our Lebanese population samples is larger than that reported in any other published study.

For Tomaszewska et al.[23] and Piagkou et al.,[24] the average anteroposterior diameter of the GPF was 5.0 ± 0.4 and 5.3 ± 0.9 mm, respectively.

Sharma and Garud[25] in their study conducted on 100 dried adult Indian skulls found that the anteroposterior dimension of the GPF varied over a very wide range of values (1.68–14.94 mm) with a mean of 4.72 ± 1.40 mm.

According to a systematic review including 24 studies,[7] average values for the anteroposterior diameter of the GPF

Table 5: Summary and test statistics for greater palatine canal diameter of upper and lower openings, diameter of curvature and length, by gender

	Males		Females		Mean difference	SE difference	95% CI of difference		t statistic	P
	n	Mean ± SD	n	Mean ± SD			Lower	Upper		
Diameter upper opening (mm)										
Right	41	6.36 ± 1.33	38	5.31 ± 0.85	1.045	0.254	0.540	1.551	4.115	<0.001*
Left	41	6.10 ± 1.26	38	5.53 ± 1.23	0.566	0.281	0.006	1.125	2.014	0.048*
Diameter lower opening (mm)										
Right	41	6.78 ± 1.26	38	5.98 ± 1.19	0.800	0.276	0.249	1.350	2.892	0.005*
Left	41	6.65 ± 1.05	38	6.17 ± 1.08	0.483	0.242	0.001	0.965	1.997	0.049*
Diameter of curvature (mm)										
Right	32	2.49 ± 0.75	32	2.32 ± 0.67	0.172	0.178	−0.184	0.527	0.964	0.339
Left	32	2.52 ± 0.52	27	2.37 ± 0.58	0.157	0.143	−0.130	0.443	1.094	0.278
GPC length (mm)										
Right	41	35.49 ± 3.99	38	34.52 ± 3.77	0.273	0.966	−0.777	2.709	1.104	0.273
Left	41	35.60 ± 3.91	38	34.38 ± 3.67	0.16	1.212	−0.490	2.914	1.418	0.160

*Statistically significant at P<0.05. GPC: Greater palatine canal, SD: Standard deviation, CI: Confidence interval

Table 6: Summary and test statistics for the intracanal curvature location, by gender

	Lower	Middle	Absent	Upper	Chi-square statistic	P
Right (%)						
Male	1 (1.3)	23 (29.1)	9 (11.4)	8 (10.1)	1.12[†]	0.859[†]
Female	1 (1.3)	25 (31.6)	6 (7.6)	6 (7.6)		
Left (%)						
Male	1 (1.3)	25 (31.6)	10 (12.7)	5 (6.3)	5.635[†]	0.108[†]
Female	2 (2.5)	14 (17.7)	11 (13.9)	11 (13.9)		

[†]Fisher's exact test and significance reported instead of Chi-square because of a violation of minimum expected cell count requirement

range from 4.5 to 5.3 mm, which is lower than our mean for the entire sample but closer to the one of our female subsample.

Whereas the upper opening diameter of the GPC-PPF component, to the best of our knowledge, it was not reported in the literature yet, especially the studies which took the total height of the PPF to consider the upper limit. In our sample, the measurements ranged from 3.22 to 9.8 mm.

Finally, some limiting factors exist in our study such as (1) The small number of CBCT scans evaluated making necessary further studies to be performed on a larger group of patients which can lead to more accurate results; (2) Our sample of Lebanese population concerns only the adults making the results nonapplicable to younger generations; (3) In our study, we did not take into consideration the anatomical body/cranial size of the patients, something that would be subsequently of interest to be studied.

CONCLUSION

Our study aiming to describe the morphology of the component, GPC-PPF, in a Lebanese population, using CBCT is not without limitations. Although intra-examiner reliability was high to very high for most measurements,

confirmation is pending until future research validates our findings.

Knowing that the length of the GPC and the height of the PPF are very important parameters to success the maxillary nerve block technique and to reduce potential complications, available recommendations based on published studies may not be applicable to the Lebanese population; in this respect, it is to be noted that a CBCT is imperative to analyze the morphology of the region prior performing the previously mentioned technique for higher success rates.

Financial support and sponsorship

Conflicts of interest
There are no conflicts of interest.

REFERENCES

1. Osborn AG. Radiology of the pterygoid plates and pterygopalatine fossa. AJR Am J Roentgenol 1979;132:389-94.
2. Aoun G, Zaarour I, Sokhn S, Nasseh I. Maxillary nerve block via the greater palatine canal: An old technique revisited. J Int Soc Prev Community Dent 2015;5:359-64.
3. Hwang SH, Seo JH, Joo YH, Kim BG, Cho JH, Kang JM. An anatomic study using three-dimensional reconstruction for pterygopalatine fossa infiltration via the greater palatine canal. Clin Anat 2011;24:576-82.

4. Howard-Swirzinski K, Edwards PC, Saini TS, Norton NS. Length and geometric patterns of the greater palatine canal observed in cone beam computed tomography. Int J Dent 2010;2010. pii: 292753.

5. Sved AM, Wong JD, Donkor P, Horan J, Rix L, Curtin J, et al. Complications associated with maxillary nerve block anaesthesia via the greater palatine canal. Aust Dent J 1992;37:340-5.

6. Methathrathip D, Apinhasmit W, Chompoopong S, Lertsirithong A, Ariyawatkul T, Sangvichien S. Anatomy of greater palatine foramen and canal and pterygopalatine fossa in Thais: Considerations for maxillary nerve block. Surg Radiol Anat 2005;27:511-6.

7. Tomaszewska IM, Kmiotek EK, Pena IZ, Sredniawa M, Czyzowska K, Chrzan R, et al. Computed tomography morphometric analysis of the greater palatine canal: A study of 1,500 head CT scans and a systematic review of literature. Anat Sci Int 2015;90:287-97.

8. Wormald PJ, Athanasiadis T, Rees G, Robinson S. An evaluation of effect of pterygopalatine fossa injection with local anesthetic and adrenalin in the control of nasal bleeding during endoscopic sinus surgery. Am J Rhinol 2005;19:288-92.

9. Wormald PJ, Wee DT, van Hasselt CA. Endoscopic ligation of the sphenopalatine artery for refractory posterior epistaxis. Am J Rhinol 2000;14:261-4.

10. Malamed SF, Trieger N. Intraoral maxillary nerve block: An anatomical and clinical study. Anesth Prog 1983;30:44-8.

11. Lepere AJ. Maxillary nerve block via the greater palatine canal: New look at an old technique. Anesth Pain Control Dent 1993;2:195-7.

12. Wong JD, Sved AM. Maxillary nerve block anaesthesia via the greater palatine canal: A modified technique and case reports. Aust Dent J 1991;36:15-21.

13. Douglas R, Wormald PJ. Pterygopalatine fossa infiltration through the greater palatine foramen: Where to bend the needle. Laryngoscope 2006;116:1255-7.

14. Poore TE, Carney MT. Maxillary nerve block: A useful technique. J Oral Surg 1973;31:749-55.

15. Ikuta CR, Cardoso CL, Ferreira-Júnior O, Lauris JR, Souza PH, Rubira-Bullen IR. Position of the greater palatine foramen: An anatomical study through cone beam computed tomography images. Surg Radiol Anat 2013;35:837-42.

16. Urbano ES, Melo KA, Costa ST. Morphologic study of the greater palatine canal. J Morphol Sci 2010;27:102-4.

17. Sheikhi M, Zamaninaser A, Jalalian F. Length and anatomic routes of the greater palatine canal as observed by cone beam computed tomography. Dent Res J (Isfahan) 2013;10:155-61.

18. Das S, Kim D, Cannon TY, Ebert CS Jr., Senior BA. High-resolution computed tomography analysis of the greater palatine canal. Am J Rhinol 2006;20:603-8.

19. Rapado-González O, Suárez-Quintanilla JA, Otero-Cepeda XL, Fernández-Alonso A, Suárez-Cunqueiro MM. Morphometric study of the greater palatine canal: Cone-beam computed tomography. Surg Radiol Anat 2015;37:1217-24.

20. McKinney KA, Stadler ME, Wong YT, Shah RN, Rose AS, Zdanski CJ, et al. Transpalatal greater palatine canal injection: Radioanatomic analysis of where to bend the needle for pediatric sinus surgery. Am J Rhinol Allergy 2010;24:385-8.

21. Asha ML, Arun Kumar G, Sattigeri Anupama V, Raja Jigna V, Diksha M. Cone beam computed tomographic analysis of anatomical variations of greater palatine canal and foramen in relation to gender in South Indian population. Oral Health Dent Manag 2015;14:384-90.

22. Aoun G, Nasseh I, Sokhn S, Saadeh M. Analysis of the greater palatine foramen in a Lebanese population using cone-beam computed tomography technology. J Int Soc Prev Community Dent 2015;5 Suppl 2:S82-8.

23. Tomaszewska IM, Tomaszewski KA, Kmiotek EK, Pena IZ, Urbanik A, Nowakowski M, et al. Anatomical landmarks for the localization of the greater palatine foramen – A study of 1200 head CTs, 150 dry skulls, systematic review of literature and meta-analysis. J Anat 2014;225:419-35.

24. Piagkou M, Xanthos T, Anagnostopoulou S, Demesticha T, Kotsiomitis E, Piagkos G, et al. Anatomical variation and morphology in the position of the palatine foramina in adult human skulls from Greece. J Craniomaxillofac Surg 2012;40:e206-10.

25. Sharma NA, Garud RS. Greater palatine foramen – Key to successful hemimaxillary anaesthesia: A morphometric study and report of a rare aberration. Singapore Med J 2013;54:152-9.